A major purpose of the Techni-
Information Center is to provide
broadest dissemination possi-
of information contained in
E's Research and Development
orts to business, industry, the
demic community, and federal,
e and local governments.

Although a small portion of this
ort is not reproducible, it is
g made available to expedite
availability of information on the
earch discussed herein.

1

PORTIONS OF THIS REPORT ARE ILLEGIBLE.

It has been reproduced from the best available copy to permit the broadest possible availability.

COO-3539-27

(LA-UR-84-2411)

A PROGRESS REPORT ON RECENT RARE MUON DECAY EXPERIMENTS AT THE LOS ALAMOS MESON PHYSICS FACILITY

G. E. HOGAN, R. D. BOLTON, J. D. BOWMAN, R. CARLINI, M. D. COOPER, M. DUONG-VAN[a], J. S. FRANK, A. L. HALLIN, P. HEUSI, C. M. HOFFMAN, F. G. MARIAM, H. S. MATIS[b], R. E. MISCHKE, D. E. NAGLE, V. D. SANDBERG, G. H. SANDERS, U. SENNHAUSER[c], R. L. TALAGA[d], R. WERBECK, and R. A. WILLIAMS

Los Alamos National Laboratory, Los Alamos, NM 87545

LA-UR--84-2411

DE85 001503

S. L. WILSON, E. B. HUGHES, and R. HOFSTADTER

Hansen Laboratories and Department of Physics
Stanford University, Stanford, CA 94305

D. GROSNICK and S. C. WRIGHT

University of Chicago, Chicago, IL 60637

V. L. HIGHLAND

AC02-76ER03539

Temple University, Philadelphia, PA 19122

A search has been performed for the decays $\mu \to eee$, $\mu \to e\gamma$, and $\mu \to e\gamma\gamma$ with a sensitivity in the branching ratios at the level of 10^{-10}. The experiment used a separated, 26 MeV/c μ^+ beam with an average intensity of 300kHz. A total of 2.2×10^{11} muon decays were examined for the present result. The detector for the experiment is the Crystal Box, which consists of a cylindrical drift chamber surrounded by 396 NaI(Tl) crystals. A layer of scintillation counters in front of the crystals provided timing for electrons and a veto for photons. The energy resolution for electrons and photons is ~6% (FWHM). The position resolution of the drift chamber is 350 μm leading to a vertex cut with a rejection of 10^3 for $\mu \to eee$. The timing resolution is ~300 ps from the scintillators and ~1 ns from the crystals. No candidate for $\mu \to eee$ has been found, yielding an upper limit for the branching ratio of $B_{\mu 3e} < 1.3 \times 10^{-10}$ (90% C.L.).

[a] Present address: Lawrence Livermore Laboratory, Livermore, CA
[b] Present address: Lawrence Berkeley Laboratory, Berkeley, CA
[c] Present address: SIN, Villigen, Switzerland
[d] Present address: University of Maryland, College Park, MD

MASTER

DISTRIBUTION OF THIS DOCUMENT IS UNLIMITED

1. INTRODUCTION

The muon has been a mystery since its discovery in 1937 (Ref. 1). After its properties were disentangled from the pion, physicists found a particle that could only be distinguished from the electron by its mass. In the years since, physicists have also found it necessary to distinguish between muons, electrons, and taus by invoking separate conserved additive lepton quantum numbers[2]. These quantities do not relate to any known space-time symmetry as does energy, nor to any known massless gauge boson, as does the electric charge. We know of no fundamental reason why the muon, electron, and tau family numbers should be conserved.

Present theoretical thought includes the origin of the family number problem under the hierarchy problem: Why are there more quarks and leptons beyond the u and d quarks and the electron and ν_e leptons, and what are the connections to the "extra" hierarchies? In this particular experiment, we ask how the muon and electron are connected and at what level, if any, do the neutrinoless family number violating decays $\mu \to e\gamma$, $\mu \to e\gamma\gamma$, and $\mu \to eee$ occur. The standard model is silent on this question[3]. Extensions to the standard model speak with many different voices with as many different answers[4]. Examples include the existence of multiple Higgs doublets[5]; flavor-changing neutral gauge bosons (for example, the gauge bosons associated with horizontal gauge interactions[6], or the gauge bosons present in extended technicolor theories[7]); composite models[8]; muon-number violation mediated by light lepto-quarks (present in some grand unified theories[9] and in extended technicolor theories[7]); muon-number violation mediated by supersymmetric partners of the usual $SU(2)_L \times U(1)$ gauge bosons[10]; and the existence of new electroweak interactions[11]. In general, these different sources of lepton number nonconservation predict different relative strengths for the various neutrinoless transitions. This underscores the importance of searching for all of these processes.

Another process which violates lepton-family number is neutrino oscillation[12]. Oscillations explicitly require massive neutrinos while this is not the case for the processes discussed above. However, oscillation experiments can be sensitive to very small neutrino masses (<1 eV), while effects in the neutrinoless transitions caused by these oscillations alone would be negligibly small.

Amongst this babble, the experimental limits on these decays have been steadily decreasing. See Figure 1. The current limits (90% C.L.) for the various lepton-number nonconserving decays are:

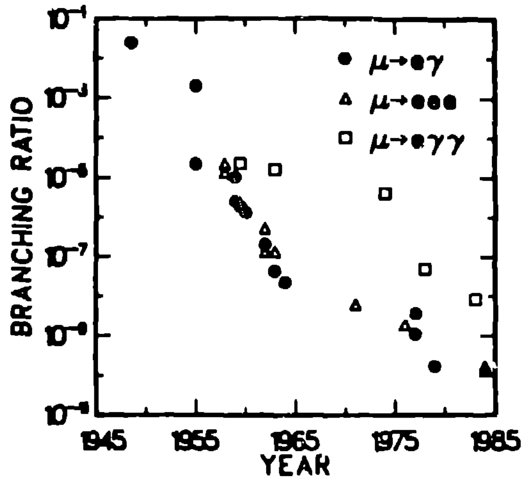

FIGURE 1
Upper limit for several muon-violating processes as function of time.

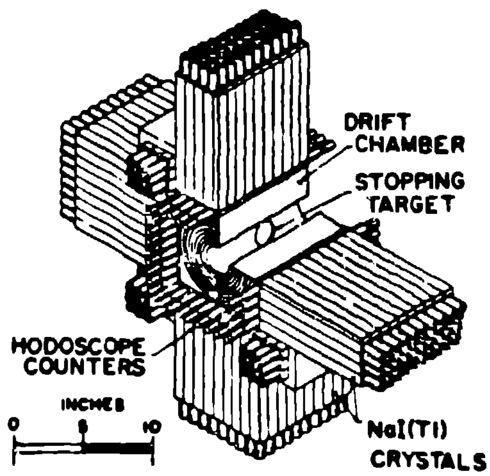

FIGURE 2
A schematic diagram of the Crystal Box detector.

$$\frac{\Gamma(\mu\to e\gamma)}{\Gamma(\mu\to e\nu\bar{\nu})} < 1.7 \times 10^{-10} \qquad \text{(Ref. 13)}$$

$$\frac{\Gamma(\mu\to eee)}{\Gamma(\mu\to e\nu\bar{\nu})} < 1.6 \times 10^{-10} \qquad \text{(Ref. 14)}$$

$$\frac{\Gamma(\mu\to e\gamma\gamma)}{\Gamma(\mu\to e\nu\bar{\nu})} < 8.4 \times 10^{-9} \qquad \text{(Ref. 15)}$$

2. THE EXPERIMENTAL HARDWARE

The Crystal Box detector is designed to improve the limits on each of these decays to the level of 10^{-11}. It is shown in Figure 2. It is a general purpose charged particle and photon detector of large solid angle in place at the Stopped Muon Channel of the Clinton P. Anderson Meson Physics Facility (LAMPF). A separated, 26 MeV/c μ^+ beam stops in an elliptical, polystyrene target located at the center of the detector. The target tilts at 45° with respect to the beam direction to present a 6.7 cm radius projected circular cross section, 52 mg/cm^2 thick, to the beam. The muon stopping rate is typically 3×10^5 s^{-1} (average) with a duty factor of 6.8%. The polarization of decaying muons in polystyrene is measured to be (14.6 ± 1.4)%. Surrounding the target is a 728-wire, eight-plane, large-stereo-angle drift chamber,[16] which determines the tracks of charged particles in three dimensions. The single-plane resolution is about 350 μm FWHM. The measured single track tion efficiency is 95%. The chamber presents an average of ^{3} radiation lengths to a particle traversing it in a direction the beam axis. There is no applied magnetic field. The knowledge igin and the original direction of a charged particle is limited by scattering in the target, the target frame, and the inner ber foil. The position resolution of the origin on the target is on of 2 mm.

particles next traverse a scintillator hodoscope containing 36 Each counter is 44.5 × 5.7 × 1.27 cm, with a photomultiplier each end by a light pipe. These counters define the fiducial charged particles. The counters also provide timing and position n. Constant fraction discriminator[17] signals from the two ends of a or are connected to a meantimer[18] for trigger coincidence decisions. ed time resolution of each counter is 290 ps (FWHM). The position along the length of the counter is 4.2 cm (FWHM).

gions upstream and downstream of the hodoscope are covered by 16 veto ion counters, each measuring 13.3 × 23.8 × 0.3 cm. These counters to help distinguish charged particles from photons. Their average lution is 750 ps (FWHM).

itermost part of the dete r is an array of 360 NaI(Tl) face 6.35 × 6.35 cm cross section and 30.5 cm long, plus 36 corner 6.35 × 6.35 × 63.5 cm. These crystals are packaged in a single lly sealed container. Paper wrapping around each crystal provides solation. Each face crystal is coupled to a single photomultiplier e corner crystals have photomultipliers at both ends. Each iplier has its own constant fraction discriminator with a threshold

isolute energy gain of each NaI(Tl) crystal is calibrated using a source (4.43 MeV γ) and the reactions $\pi^- p \to n\pi^0(\to\gamma\gamma)$ $\leq$ 83 MeV) and $\pi^- p \to n\gamma$ (E_γ = 129.4 MeV). The measured energy n function is approximately an asymmetric gaussian with a FWHM of 30 MeV. See Figure 3. The pion data is taken with a liquid hydrogen placing the drift chamber.

ins and offsets for the timing system are calibrated using Michel itrons coming from a centrally placed plastic counter just behind the The coincidence of this counter with the scintillator hodoscope and orms a timing trigger with the timing start signal advanced 10 ns on ier trigger. The alternating start signal provides a calibration of the gain of the timing system. The NaI was calibrated once during our January run, the plastic scintillators were calibrated daily.

The stability of the gains of each timing and pulse height NaI(Tl) channel is monitored every two hours using a Xe flash tube with a fiber optics cable connected to each photomultiplier. The timing resolution of the NaI(Tl) detectors is 1.1 ns (FWHM). The photon conversion point is determined to about 3.8 cm (FWHM) by the energy sharing in the different NaI crystals.

The single particle acceptance in the fiducial area (which assures shower containment in the NaI(Tl)) is $\Omega/4\pi = 45\%$, including finite target-size effects. The solid angle times efficiency is approximately 12% for 3e events, 40% for $e\gamma$ events, and 14% for $e\gamma\gamma$ events. Figure 4 summarizes the sensitivity of the experiment as a function of running time and beam intensity.

3. TRIGGER REQUIREMENTS AND DATA ACQUISITION

In order to reduce the data stream to manageable proportions, the trigger of the experiment is quite complex[19]. The $e\gamma$ and $e\gamma\gamma$ triggers define particle types by quadrants. We define an electron (or positron) quadrant as a signal in a hodoscope scintillator with one or more NaI crystals in the same quadrant having more than 5 MeV. A photon quadrant is 5 MeV or more energy in at least one NaI crystal with no energy in the plastic scintillators in that quadrant. The $e\gamma$ trigger requires opposite electron and photon quadrants within 7 ns of

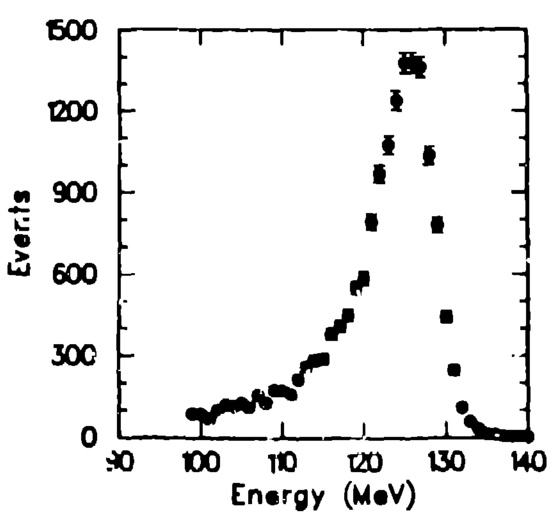

FIGURE 3
The spectrum of energy detected in the NaI(Tl) for photons from the reaction $\pi^- p \rightarrow n\gamma$.

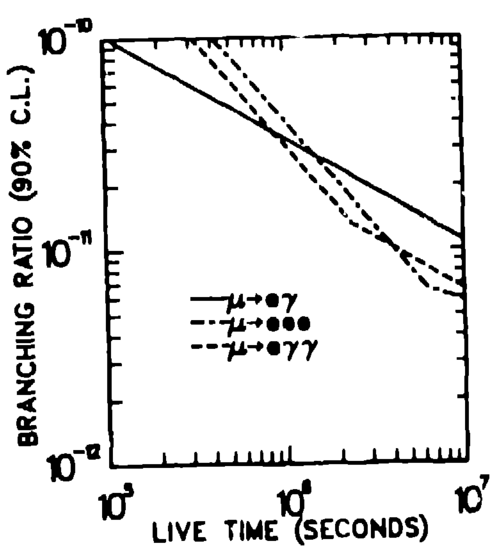

FIGURE 4
Monte Carlo prediction of branching ratio sensitivity as a function of running time for a 500KHz stopping rate.

is monitored every two hours using a Xe flash tube with a fibe
connected to each photomultiplier. The timing resolution of
detectors is 1.1 ns (FWHM). The photon conversion point is
about 3.8 cm (FWHM) by the energy sharing in the different NaI c

The single particle acceptance in the fiducial area (which
containment in the NaI(Tl)) is $\Omega/4\pi = 45\%$, including finit
effects. The solid angle times efficiency is approximately 12%
40% for eγ events, and 14% for eγγ events. Figure 4 s
sensitivity of the experiment as a function of running t
intensity.

3. TRIGGER REQUIREMENTS AND DATA ACQUISITION

In order to reduce the data stream to manageable proportion
of the experiment is quite complex[19]. The eγ and eγγ triggers d
types by quadrants. We define an electron (or positron) quadra
in a hodoscope scintillator with one or more NaI crystals in the
having more than 5 MeV. A photon quadrant is 5 MeV or more ener
one NaI crystal with no energy in the plastic scintillators in
The eγ trigger requires opposite electron and photon quadrants

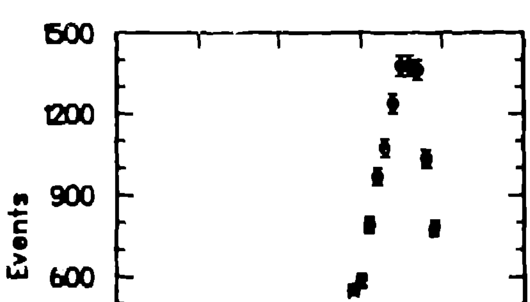

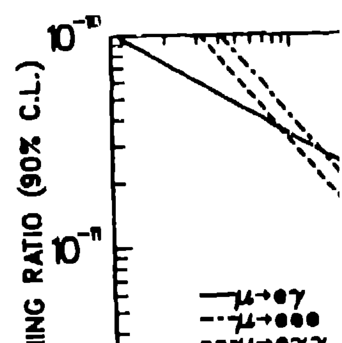

:, and that each have an NaI energy greater than 35 MeV. The $e\gamma\gamma$ equires at least two gamma quadrants, one and only one electron and a total in all of the NaI of more than 70 MeV.

trigger is much more sophisticated. It requires that three ors fire within 5 ns of each other and that there be signals in -adjacent scintillators within 15 ns of each other. When these are met, a pre-trigger starts the data acquisition system. A ost-trigger then considers the geometry of the event in detail. The er defines an electron as a signal in a hodoscope scintillator with 5 MeV of energy in a crystal in one of the three rows of crytals ehind that scintillator. The three electrons must be in a geometric inematically consistent with a 3e decay. This post-trigger takes an 150 ns. In addition, for most of the run, the post-trigger a 70 MeV threshold from the sum of all of the NaI. These three modes generate a trigger rate of about 5 Hz with a 4.4 MHz eous muon stopping rate in the target at a 6.7% duty factor (300 kHz

paratus is instrumented with analog-to-digital converters (ADC's) and igital converters (TDC's) on all of the plastic scintillators and NaI The drift-chamber wire signals are discriminated and used to stop l TDC's. In addition, a second ADC with a different gate is used on crystals as a pileup rejector. The trigger starts all the TDC's, a gate for the ADC's, and provides a start signal for the readout of :. For each event all the scintillator, ADC, and TDC data are Distributed processors are used to perform a sparse data scan for t-chamber TDC information and the NaI pulse height and timing on. Taking data in this fashion makes each event about 500 16-bit ng. At fixed intervals a number of scalers are read out; these nformation about the number of muons stopped, the duty factor, and :. A PDP-11/44 is used to acquire and tape the data. The option reduce the taping rate by using the data acquisition computer to on the data before taping.

TS

mits on the sensitivity of this experiment are determined by how well grounds are suppressed and the number of muons stopped. The sources ground are random coincidences between Michel positrons and hlung and annihilation photons, and the prompt processes $\mu \to eee\nu\bar{\nu}$, and $\mu \to e\gamma\gamma\nu\bar{\nu}$. Using the energy, time, and position resolutions one places the requirement on all decay modes that the particles be in time, that the total energy be equal to that of the muon, and that the vector sum of the momenta be zero. In addition, for 3e events, one can require that all tracks have a common origin on the target. The backgrounds are completely suppressed for the 3e and $e\gamma\gamma$ modes. Randoms dominate the background for the $e\gamma$ mode with about a 10% prompt background.

A small amount of data was collected this January. We acquired data at about 300 kHz of muons and 6.8% duty factor. Approximately 2.2×10^{11} muons were stopped. All the data were processed by a multistage filtering process. A first pass consisted of software timing cuts and geometrical cuts that could be applied without using the drift chamber reconstruction routines. This reduced the amount of data by a factor of ~10. A second pass used the drift chamber tracks to allow one to do more severe timing and geometrical cuts, and provided a further reduction of a factor of ~10. The data remaining after the first two passes consist of 10^3-10^4 events in each of the data streams. These are carefully investigated to look for a prompt signal and any candidates for lepton family violating decays. The final analysis of the $e\gamma$ and $e\gamma\gamma$ modes is still in progress. The rest of this paper will deal with the 3e mode.

The signature for a $\mu^+ \to e^+e^+e^-$ event is that the three trajectories should emerge from a common vertex in the target in time coincidence, ΣE, the sum of the three energies deposited in the NaI(Tl) plus the ionization energy losses in other materials should equal the muon mass, and the vector sum of the three momenta ($|\Sigma\vec{p}|$) should be zero.

The main source of triggers is the random coincidence of positrons from three independent ordinary muon decays. These events tend not to satisfy any of the above constraints. Events due to $\mu^+ \to e^+e^+e^-\nu_e\bar{\nu}_\mu$, a process which does not violate separate lepton number conservation, have $\Sigma E + |\Sigma\vec{p}| < M_\mu$ and ΣE generally much less than M_μ.

The first analysis pass requires that three non-adjacent scintillator meantimes occur within a 1.5 ns interval, and that each of these scintillators have behind it a NaI(Tl) clump with at least 10 MeV within a 5 ns interval. A clump is defined as the crystal with the largest local pulse height plus the nearest 24 surrounding crystals. The output of the first pass is 1.3×10^5 events.

For the second pass, we reconstruct tracks in the drift chamber that intersect the active scintillators. The reconstruction program requires hits in at least 7 of the 8 drift chamber layers for each track. The analysis requires that three tracks intersect the target plane with an angle of more than 3°, and that the rms sum of the distances between the three track intersection points on the target (the vertex) must be less than a radius of 6 cm. Finally, a cut $\Sigma E + |\Sigma\vec{p}| < 120$ MeV, is imposed. A total of 3112 events survive these cuts.

The third analysis pass tightens the vertex cut after weighting each track-target intersection point according to the uncertainty in the measurement of that point. The 1.5 ns scintillator timing cut is reimposed after correcting each particle's time-of-flight for the path length from the vertex to the scintillator. This pass reduces the number of events to 83.

The final cuts require that $\Sigma E + |\Sigma\vec{p}| < 110$ MeV, $|\Sigma\vec{p}| < 12$ MeV, and that the three scintillator meantimes occur within a 1 ns interval. No events pass these cuts. The acceptance of the apparatus was calculated with a Monte Carlo program that accurately reproduces the response of the detectors to positrons, electrons, and photons. Electromagnetic showers are simulated with the shower code EGS (Ref. 20). The product of the acceptance and detector efficiency for $\mu \to 3e$ events, assuming a constant matrix element, is (8.5 ± 0.8%). We obtain an upper limit of

$$B_{\mu 3e} < 1.3 \times 10^{-10} \text{ (90\% C.L.)} \quad .$$

As a check of the performance of the apparatus and the normalization, the portion of the data taken without the total NaI energy requirement (2.55×10^{10} muons stopped) was analyzed for $\mu^+ \to e^+e^+e^-\nu_e\bar{\nu}_\mu$ events. Since these events tend to have a non-zero vector momentum sum, the $|\Sigma\vec{p}|$ cut was removed. Eleven events passed these cuts. The Monte Carlo program predicts 12 ± 2 events, using a matrix element based on standard electroweak theory[21]. The distributions of ΣE, $\Sigma E + |\Sigma\vec{p}|$, vertex, and timing for the data and the Monte Carlo events agree with each other. The agreement of these distributions and of the number of events, verifies the validity of the assumed detector resolutions efficiencies, calibrations, and the beam normalization. Figure 5a shows the distribution of ΣE vs. $\Sigma|\vec{p}|$ for the detected $\mu^+ \to e^+e^+e^-\nu_e\bar{\nu}_\mu$ events and a 90% acceptance contour for $\mu^+ \to e^+e^+e^-$ events. Figure 5b shows the unnormalized distribution for $\mu^+ \to e^+e^+e^-\nu_e\bar{\nu}_\mu$ events from the Monte Carlo simulation.

It is expected that we will take data representing 10^{12} stopped muons this summer, and that limits of 10^{-11} will be placed on all three decay modes.

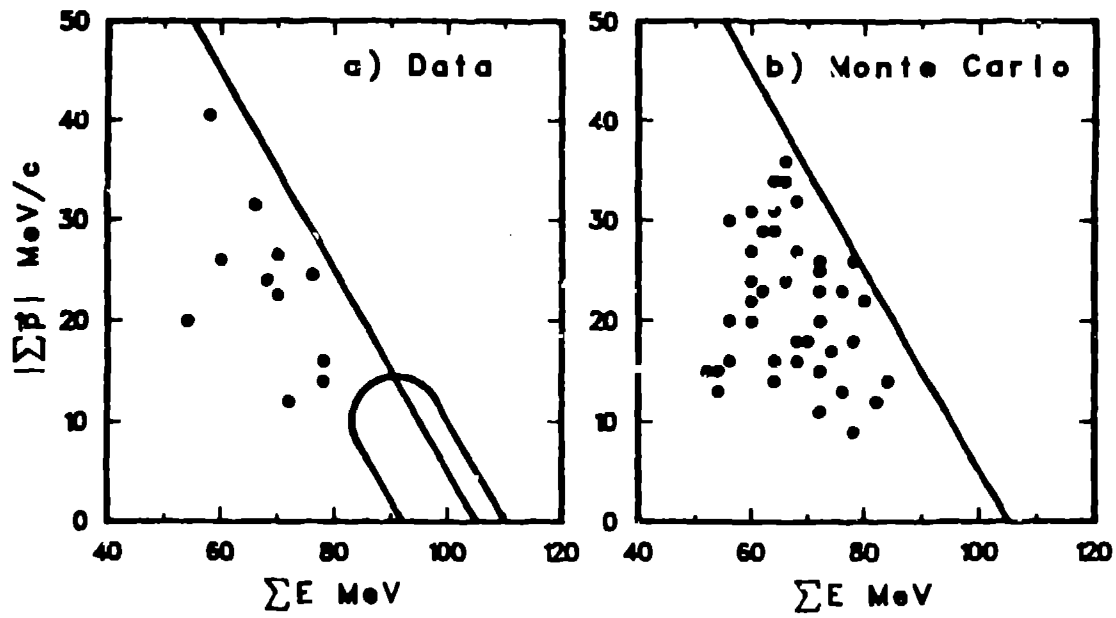

FIGURE 5a FIGURE 5b

5a. The vector sum of the momenta for the two positrons and the electron ($|\Sigma\vec{p}|$) vs. the sum of their energies (ΣE) for data events. The sloping line represents the condition $\Sigma E + |\Sigma\vec{p}| = M_\mu$. The area enclosed near $\Sigma E = 100$ MeV, $|\Sigma\vec{p}| = 0$ contains 90% of Monte Carlo $\mu^+ \to e^+e^+e^-$ events.

5b. The distribution of Monte Carlo $\mu^+ \to e^+e^+e^-\nu_e\bar{\nu}_\mu$ events.

ACKNOWLEDGEMENT

A large experiment such as this would not be possible without the contributions of many people. In particular we would like to thank L. Bayliss, H. Butler, S. Chesney, R. Damjanovich, L. G. Doster, M. Dugan, C. Espinoza, T. Gordon, G. Hart, R. Parks, R. Poe, J. Rolfe, J. Sandoval, H. P. von Guten, and H. Zeman. In addition, we would like to thank the LAMPF staff for their many contributions and L. Rosen for his continuing support of this experiment. This work was supported in part by the US Department of Energy and the National Science Foundation.

REFERENCES

1) C. D. Andersen and S. H. Neddermeyer, Phys. Rev. 51, 884 (1937); and J. C. Street and E. Stevensen, Phys. Rev. J., 1005 (1937).

2) J. Schwinger, Ann. Phys. 2, 407 (157); K. Nishijima, Phys. Rev. 108, 907 (1957); and S. Bludman, Nuovo Cim. 9, 433 (1958).

3) S. L. Glashow, Nucl. Phys. 22, 579 (1961); A. Salam, in Elementary Particle Theory: Relativistic Groups and Analyticity (Nobel Symposium No. 8), edited by N. Svartholm (Almqvist and Wiksell, Stockholm, 1968), p. 367; S. Weinberg, Phys. Rev. Lett. 19, 1264 (1967).

4) C. M. Hoffman, LA-UR-84-1327, to be published in the Proceedings of the 4th Course of the International School of Physics of Exotic Atoms on Fundamental Interactions in Low Energy systems, Erice, Italy, March 31-April 6, 1984.

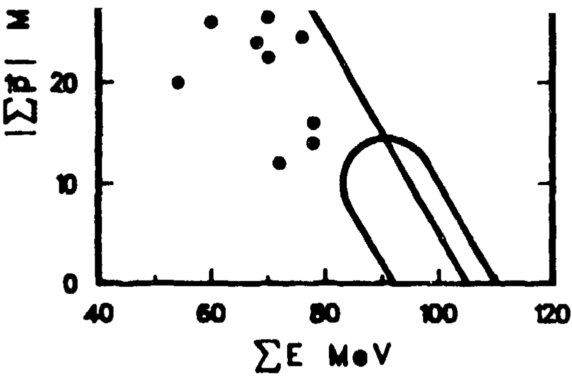

FIGURE 5a

5a. The vector sum of the momenta
($|\Sigma\vec{p}|$) vs. the sum of their energies (
represents the condition $\Sigma E + |\Sigma$
$\Sigma E = 100$ MeV, $|\Sigma\vec{p}| = 0$ contains 90% of

5b. The distribution of Monte Carlo

ACKNOWLEDGEMENT

A large experiment such as this
contributions of many people. In
L. Bayliss, H. Butler, S. Chesney, I
C. Espinoza, T. Gordon, G. Hart, R.
H. P. von Guten, and H. Zeman. In add
staff for their many contributions and
this experiment. This work was supp
Energy and the National Science Founda

5) J. D. Bjorken and S. Weinberg, Phys. Rev. lett. 38, 622 (1977); and G. C. Branco, Phys. Lett. 68B, 455 (1977).

6) T. Maehara and T. Yanagida, Lett. Nuovo Cimento 19, 424 (1977), Prog. Theor. Phys. 60, 822 (1978), and Prog. Theor. Phys. 61, 1434.

7) J. Ellis, M. K. Gaillard, D. V. Nanopoulos, and P. Sikivie, Nucl. Phys. B 182, 529 (1981); S. Dimopoulos and J. Ellis, Nucl. Phys. B 182, 505 (1981); J. Ellis and P. Sikivie, Phys. Lett. 104B, 141 (1981); and A. Masiero, E. Papantonopoulos, and T. Yanagida, Phys. Lett. 115B, 229 (1982).

8) Y. Tomozawa, Phys. Rev. D 25, 1448 (1982); and E. J. Eichten, K. D. Lane, and M. E. Peskin, Phys. Rev. Lett. 50, 811 (1983).

9) V. Elias and S. Rajpoot, Phys. Rev. D 20, 2445 (1979); J. C. Pati, invited talk at the International Conference on Baryon Nonconservation, Tata Institute of Fundamental Research, Bombay, India, 1982 (University of Maryland Report 82-151, 1982). The unification scales to two loops have been calculated in these models by T. Goldman [in Particles and Fields - 1981: Testing the Standard Model, proceedings of the meeting of the Division of Particles and Fields of the APS, Santa Cruz, California, edited by C. A. Heusch and W. T. Kirk (AIP, New York, (1982))].

10) J. Ellis and D. V. Nanopoulos, Phys. Lett. 110B, 44 (1982).

11) R. N. Mohapatra and G. Senjanović, Phys. Rev. D 23, 165 (1981); and Riazuddin, R. E. Marshak, and R. N. Mohapatra, Phys. Rev. D 24, 1310 (1981).

12) See, for example, S. M. Blenky and B. Pontecorvo, Phys. Rev. 41, 225 (1978).

13) W. W. Kinnison et al., Phys. Rev. D 25, 2846 (1982)

14) W. Bertl et al., Phys. Lett. 140B, 299 (1984). The best previous result is $B_{\mu 3e} < 1.9 \times 10^{-9}$ (90% C.L.). from S. M. Korenchenko et al., JETP 43, (1976).

15) G. Azuelos et al., Phys. Rev. Lett. 51, 164 (1983).

16) Richard D. Bolton et al, Nucl. Inst. & Meth. 188, 275 (1981).

17) G. H. Sanders, G. W. Hart, G. E. Hogan, J. S. Frank, C. M. Hoffman, H. S. Matis, and V. D. Sandberg, Nucl. Inst. and Methods 180, 603 (1981).

18) V. D. Sandberg, L. S. Bayliss, M. P. Dugan, J. S. Frank, T. Gordon, et al., LA-UR-84-2019, submitted to Nucl. Inst. and Methods.

19) G. H. Sanders et al., "Intelligent Trigger Processor for the Crystal Box," in proceedings of the Topical Conference on the Application of Microprocessors to High-Energy Physics Experiments, CERN 81-07, p. 214 (1981).

20) R. L. Ford and W. R. Nelson, SLAC Report, SLAC -210 (1978) (unpublished).

21) D. Yu Bardin, Ts. G. Istathov, G. A. Mitsel'Makker, Yad Fiz 15, 284 (1972) [Sov. J. Nucl. Phys. 15, 161 (1972)]. The matrix element was evaluated by J. Sapirstein, SLAC (private communication).

DISCLAIMER

This report was prepared as an account of work sponsored by an agency of the United States Government. Neither the United States Government nor any agency thereof, nor any of their employees, makes any warranty, express or implied, or assumes any legal liability or responsibility for the accuracy, completeness, or usefulness of any information, apparatus, product, or process disclosed, or represents that its use would not infringe privately owned rights. Reference herein to any specific commercial product, process, or service by trade name, trademark, manufacturer, or otherwise does not necessarily constitute or imply its endorsement, recommendation, or favoring by the United States Government or any agency thereof. The views and opinions of authors expressed herein do not necessarily state or reflect those of the United States Government or any agency thereof.